Research Article

Cracking Behaviors and Mechanical Properties of Rock-Like Specimens with Two Unparallel Flaws under Conventional Triaxial Compression

Huilin Le [ID],[1] Shaorui Sun [ID],[2] Chenghua Xu,[1] Liuyang Li [ID],[1] and Yong Liu [ID][1]

[1]*Ph.D. Candidate, Department of Geology Engineering, Hohai University, Nanjing 210098, China*
[2]*Professor, Department of Geology Engineering, Hohai University, Nanjing 210098, China*

Correspondence should be addressed to Huilin Le; lehuilin@hhu.edu.cn and Shaorui Sun; sunsrhhu@163.com

Flaws existing in rock masses are generally unparallel and under three-dimensional stress; however, the mechanical and cracking behaviors of the specimens with two unparallel flaws under triaxial compression have been rarely studied. Therefore, this study conducted comprehensive research on the cracking and coalescence behavior and mechanical properties of specimens with two unparallel flaws under triaxial compression. Triaxial compressive tests were conducted under different confining pressures on rock-like specimens with two preexisting flaws but varying flaw geometries (with respect to the inclination angle of the two unparallel flaws, rock bridge length, and rock bridge inclination angle). Six crack types and eleven coalescence types in the bridge region were observed, and three types of failure modes (tensile failure, shear failure, and tensile-shear failure) were observed in experiments. Test results show that bridge length and bridge inclination angle have an effect on the coalescence pattern, but the influence of bridge inclination angle is larger than that of the bridge length. When the confining pressure is low, coalescence patterns and failure modes of the specimens are greatly affected by flaw geometry, but when confining pressure rose to a certain level, the influence of confining pressure is larger than the effect of flaw geometry. The peak strength of the specimens is affected by flaw geometry and confining pressure. There is a critical value for the bridge length. If the bridge length is larger than the critical value, peak strengths of the samples almost keep constant as the bridge length increases. In addition, as the bridge inclination angle increases, there is an increase in the probability of tensile cracks occurring, and with an increase in the confining pressure, the probability of the occurrence of shear cracks increases.

1. Introduction

Rock masses often contain flaws such as fissures, weak surfaces, and joints, which have a significant effect on the mechanical properties and failure modes of the rock mass. As rock mass instability is usually caused by such flaws, it is thus meaningful to study the influence of flaws on the strength and failure behavior of rock masses. Many previous researchers [1–10] have conducted extensive studies on the influence of flaw length, flaw inclination angle, flaw arrangement, rock bridge length, and rock bridge angle on the strength and failure behavior of rock specimens under uniaxial compression, and such studies have provided a preliminary understanding of the mechanical properties and crack propagation mechanism of fractured rock masses under uniaxial compression.

However, as rock masses are always under three-dimensional stress, it is more realistic to study the effect of preexisting flaws on the mechanical properties and crack propagation mechanisms of rock masses under triaxial compression. Huang et al. [11] carried out triaxial compressive tests on sandstone samples with two parallel flaws, and results showed that, for the specimens with parallel flaws and small inclination angles, cracks initiated from the inner flaw tips and led to simple direct shear coalescence. However, for the specimens with parallel flaws that had a large

inclination angle, complex indirect coalescence or no coalescence appeared in the specimens. Based on the results of triaxial compressive tests, Yang et al. [12] revealed that the peak strengths and failure modes depend not only on flaw geometry but also on the confining pressure. They also found that the failure modes and deformation behavior of medium marble were dependent on crack coalescence in the specimens. Huang and Yang [13] conducted triaxial compressive tests on granite samples with two coplanar three-dimensional flaws; they identified four types of crack coalescence modes based on test results and found that shear cracks and antitensile cracks were dominant under high confining pressure and also revealed that triaxial compressive strength increased with the increasing confining pressure and flaw inclination angle. Furthermore, Liu et al. [14] carried out true triaxial compressive tests on the rock-like specimens with three collinear preexisting flaws and revealed that peak stresses of the specimens changed with flaw inclination angle and peak stresses increased as the confining pressure increases.

The above research focused on parallel flaws in the specimens. However, flaws are generally unparallel in engineering. The study about cracking behaviors and mechanical parameters of rock samples with two unparallel preexisting flaws under uniaxial compression are extensive. Lee and Jeon [7] used three materials to make different types of samples, where the flaw geometry in the sample was a combination of an inclined flaw and a horizontal flaw, and revealed that the model material had a significant effect on the crack initiation and propagation pattern of the specimens under uniaxial compression. Haeri et al. [15] studied the fracturing process of the rock-like specimens under uniaxial compression and found that the propagation of wing cracks initiated from preexisting flaws led to crack coalescence in the bridge area; they also showed that secondary cracks emanated after the initiation of the wing cracks. Huang et al. [16] conducted uniaxial compressive tests on rock-like specimens with two parallel flaws and discussed the crack propagation mechanism under microscopic observation. They also showed that the peak strength and Young's modulus of specimens firstly decreased and then increased as the flaw inclination angle increased from $0°$ to $75°$. Furthermore, the mechanical properties and failure behavior of red sandstone specimens with two unparallel flaws were studied by Yang et al. [17], who found that the mechanical parameters of the specimens were affected by the flaw inclination angle and that the cracking process depended not only on the flaw inclination angle but also on the heterogeneity of the rock material. Haeri et al. [18] studied the influence of unparallel flaws on the strength and stress-strain curves of rock-like specimens, and their experimental and numerical results revealed that the crack coalescence and final crack propagating paths were mainly caused by wing cracks.

However, the researches about strengths and cracking behaviors of rock specimens with two unparallel preexisting flaws under triaxial compression are rare and the conclusions are limited. Only Huang et al. [19] carried out triaxial compressive tests on the rock-like specimens with two

unparallel preexisting flaws and found that failure modes of the specimens were determined by both the flaw inclination angle and the confining pressure: when the confining pressure was small, failure modes were mainly affected by the flaw inclination angle, and when the confining pressure was large, failure modes were mainly influenced by the confining pressure. Therefore, in this research, rock-like specimens with two unparallel preexisting flaws were prepared, and triaxial compressive tests were conducted on these specimens under different confining pressures. The effects of confining pressure, rock bridge length, rock bridge inclination angle, and flaw inclination angle on the strengths and crack behavior of specimens under different confining pressures were then analyzed based on the test results. This paper thus provides a better understanding of the mechanical properties and failure behavior of rock masses with unparallel flaws and different flaw geometries under triaxial compression.

2. Experimental Program

2.1. Specimen Preparation. There are a number of advantages to make specimens using rock-like materials (for example, they are easy to prepare and provide repeatability of results), and they have thus been employed by many researchers [20–24]. In this research, specimens are made of a mixture of Portland cement, fine sand, and water at a ratio of $1 : 2 : 0.5$ by weight. The mixture was poured into a mold that had internal dimensions of $70\,\text{mm} \times 70\,\text{mm} \times 140\,\text{mm}$. The unparallel preexisting flaws in the specimens were fabricated by inserting two steel sheets (10 mm wide and 1 mm thick) into the mixture, resulting in a flaw with a length of 10 mm and aperture of 1 mm. Four parameters were changed to produce different geometries of these preexisting flaws (Figure 1): the inclination angle of flaw 1 α_1; the inclination angle of flaw 2 α_2; the bridge inclination angle (β); the bridge ligament length ($2b$). The bridge inclination angle, β, varied between $0°$ and $120°$ in intervals of $30°$. Four ligament lengths of $2b = 10\,\text{mm}$, 20 mm, 30 mm, and 40 mm were set; α_1 was set to $0°$ and $30°$, respectively; and α_2 was set to $60°$. Therefore, in a specimen with a geometry of 10-0-60-30, $2b$ is equal to 10 mm, α_1 is equal to $0°$, α_2 is equal to $60°$, and β is equal to $30°$. The geometries of four series of the specimens are summarized in Table 1. The mold was stored in a room at a temperature of $20°\text{C}$ for 24 h; the specimens were then removed from the mold, and the steel sheets were pulled out. The prismatic specimens were subsequently placed in a water tank for curing at a temperature of $20°\text{C}$ for 28 days and then drilled and cut. Finally, the cylindrical specimens that had a 54 mm diameter and 108 mm height with two unparallel flaws were prepared (Figure 2).

2.2. Testing. British-made equipment (Figure 3) was used to carry out triaxial compression tests on the prefissured rock-like material samples. The maximum confining pressure, maximum vertical load, and maximum axial displacement of the equipment were 70 MPa, 1560 kN, and 50 mm, respectively. The confining pressure was raised to the desired
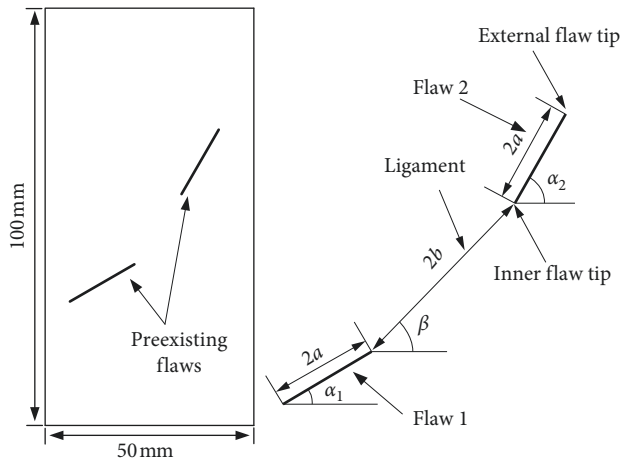
FIGURE 1: Geometry of preexisting flaws.

TABLE 1: Flaw geometries of two unparallel flaws.

Series	Lower flaw inclination angle α_1 (°)	Upper flaw inclination angle α_2 (°)	Bridging angle β (°)	Bridging length $2b$ (mm)
1	0	60	60	10, 20, 30, 40
2	30	60	60	10, 20, 30, 40
3	0	60	0, 30, 60, 90, 120	10
4	30	60	0, 30, 60, 90, 120	10

FIGURE 2: Prepared specimens with two unparallel flaws.

value (1 MPa, 2 MPa, 3 MPa, 4 MPa, and 5 MPa) at a rate of 0.2 MPa/s. A constant confining pressure was maintained, and the major principal stress was applied at a rate of 0.1 MPa/s until failure occurred.

FIGURE 3: Testing equipment for triaxial compression.

3. Results and Discussion

3.1. Crack Types in the Specimens with Different Bridge Lengths and Bridge Angles. By observing the cracks in the specimens with different bridge lengths and inclination angles, six different crack types were classified based on the crack initiation position and propagation mechanism (Figure 4). Crack type I is a tensile crack that initiates from the flaw tips and develops along the direction of the maximum principal stress. Crack type II is similar to crack type I, and the difference between these two crack types is the crack initiation position: crack type II initiates from a position close to the flaw tips. Crack type III is an antitensile crack, and crack development is the reverse of that of crack type I. Crack type IV is a "normal shear crack"; it initiates from the flaw tips, and its development direction is roughly normal to the direction of the maximum principal stress. Crack type V is a "coplanar shear crack"; it initiates from the flaw tips, and its development direction is parallel to the plane of the preexisting flaw. Crack type VI is a far-field crack that initiates from a position far away from the flaw tips, and its development direction is vertical or horizontal. Finally, crack type VI is either a tensile or shear crack.

3.2. Effect of Bridge Length on the Cracking Process, Co-alescence Pattern, and Failure Mode. Figures 5 and 6 show the failure modes of specimens with geometries of 2*b*-0-60-60 and 2*b*-30-60-60 and with different bridge lengths under 1 MPa, 3 MPa, and 5 MPa. Figure 7 shows the coalescence types of these specimens. Figure 5 shows that, for specimens with a geometry of 10-0-60-60, the type of coalescence was type 3 under different confining pressures (as shown in Figure 7). The bridge ligament length was small, and co-alescence occurred easily due to the linkage of shear cracks which initiate from the inner tips of two flaws. When the confining pressure was 1 MPa and 3 MPa, tensile cracks initiated from the external tip of flaw 2, and the failure mode of the specimens was tensile-shear failure; however, when the confining pressure was 5 MPa, the failure mode of the specimens was shear failure caused by a normal shear crack initiating from the tips of flaw 2. For specimens with a geometry of 20-0-60-60, the type 4 coalescence pattern was observed when the confining pressure was 1 MPa; tensile cracks initiated from the inner tips of two preexisting flaws
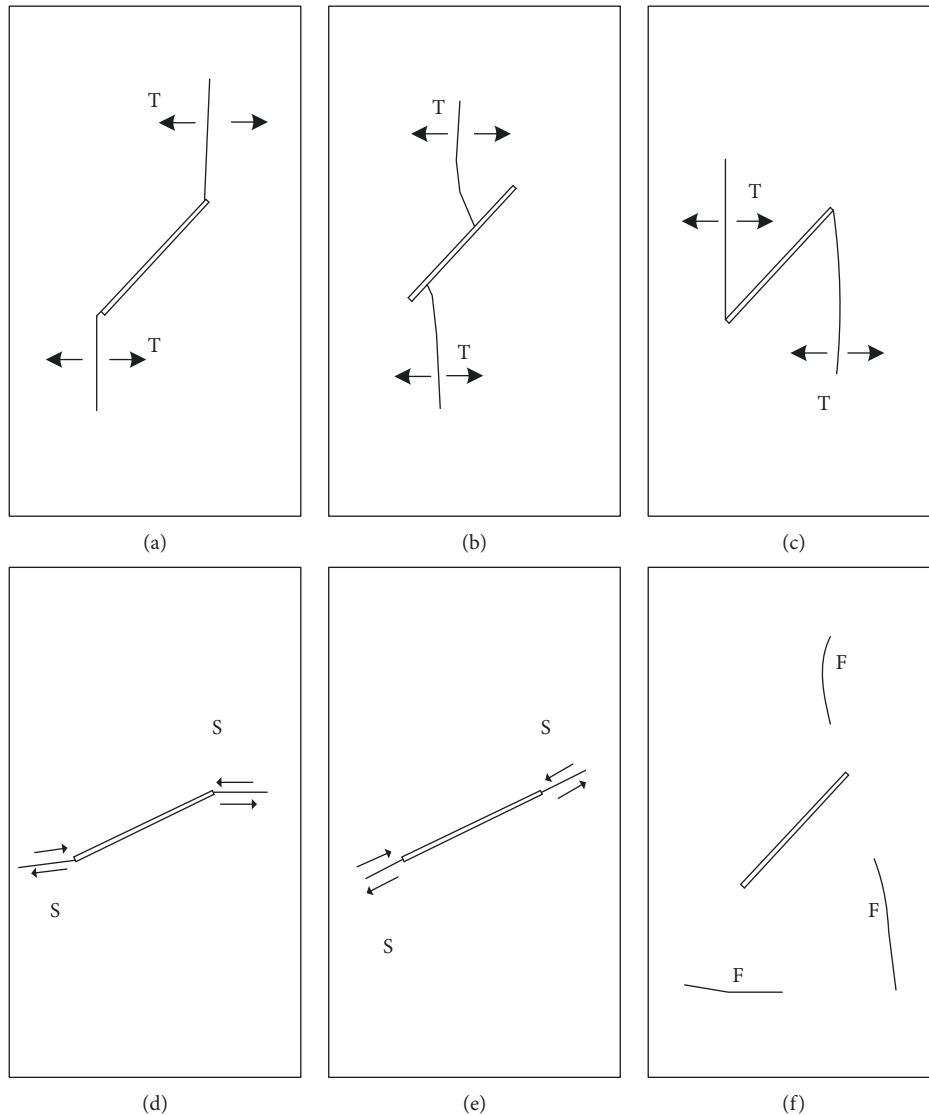
FIGURE 4: Crack types in the specimens with different bridge lengths and bridge angles: (a) tensile crack at the open flaw tip; (b) tensile crack at a position that is located close to the open flaw tip; (c) antitensile crack; (d) normal shear crack; (e) coplanar shear crack; (f) far-field crack.

and intersected with a shear crack that emanated from the center of the ligament between two inner flaw tips, which caused the rock bridge to be cut through. The failure mode of the specimens with a geometry of 20-0-60-60 was tensile-shear failure. When the confining pressure was 3 MPa and 5 MPa, type 5 coalescence pattern was observed, and tensile cracks emanated from flaw 1 with an inclination angle of 0° and intersected with shear cracks initiated from flaw 2 with an inclination angle of 60°. It indicates that shear cracks were easier to initiate from the flaw with an inclination angle of 60°. For the specimens with a geometry of 30-0-60-60, no coalescence was observed when the confining pressure was 1 MPa, and the failure mode was tensile-shear failure. When the confining pressure was 3 MPa, indirect coalescence was observed, tensile cracks initiated from the inner tip of flaw 1, and normal shear cracks initiated from the tip of flaw 2. When the confining pressure was 5 MPa, the type of co-alescence was type 3. Not the coalescence of cracks initiated

from the inner tips of flaw 1 and flaw 2, but shear cracks initiated from the external tip of flaw 1 caused the failure of the specimens. For specimens with a geometry of 40-0-60-60, no coalescence was observed when the bridge length was increased to 40 mm and the confining pressure was 1 MPa; when the confining pressure was 3 MPa, the rock bridge was cut through and caused failure of the specimen. When the confining pressure was 5 MPa, failure of the specimens was caused by a normal shear crack initiated from the inner tip of flaw 1 but was not caused by the coalescence of cracks emanating from two preexisting flaws.

Figure 6 shows that, for the specimens with a geometry of 10-30-60-60 under different confining pressures, the type of coalescence was type 3. Under confining pressures of 1 MPa and 3 MPa, the failure mode of specimens was tensile-shear failure; and under a confining pressure of 5 MPa, shear failure of the specimens was caused by a normal shear crack which initiated from the external tip of
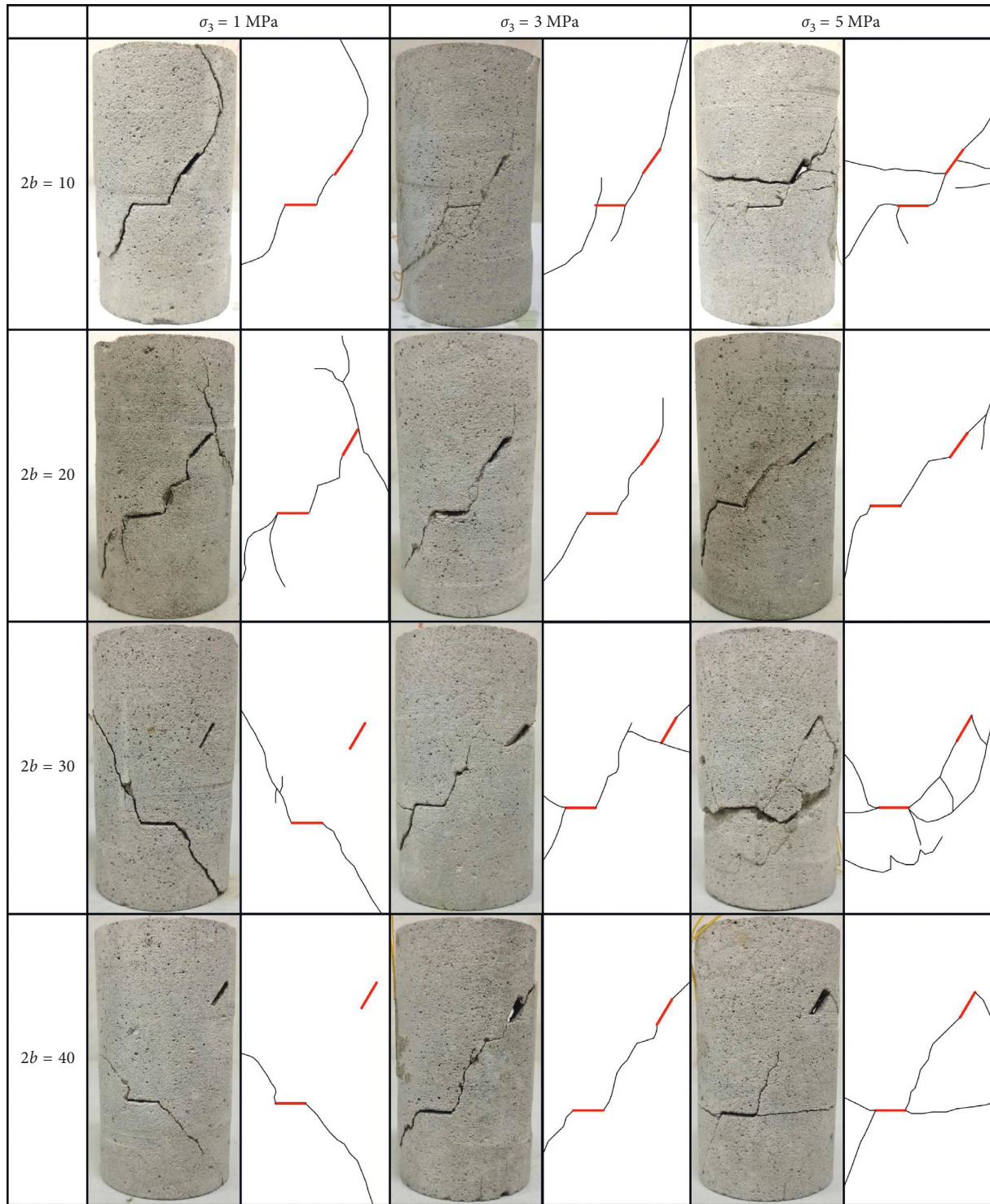
FIGURE 5: Failure modes of the specimens with a geometry of 2b-0-60-60 but with different bridge lengths.

flaw 1. Under the same confining pressure, the failure mode and coalescence pattern of these specimens were almost the same as those of specimens with a geometry of 10-0-60-60. This shows that when the bridge length is 10 mm, the change in α_1 has little influence on the failure mode and coalescence pattern of the specimen. For the specimens with a geometry of 20-30-60-60, no coalescence was observed when the confining pressure was 1 MPa, and an antitensile crack was initiated from the tip of flaw 1, which led to tensile-shear failure of the specimen. The coalescence types were the same (type 3) under confining pressures of 3 MPa and 5 MPa; however, the failure modes were different (tensile-shear failure under 3 MPa and shear failure under 5 MPa). The coalescence pattern for the specimens with a geometry of 20-30-60-60 was different from that of the specimens with a geometry of 20-0-60-60, which proves
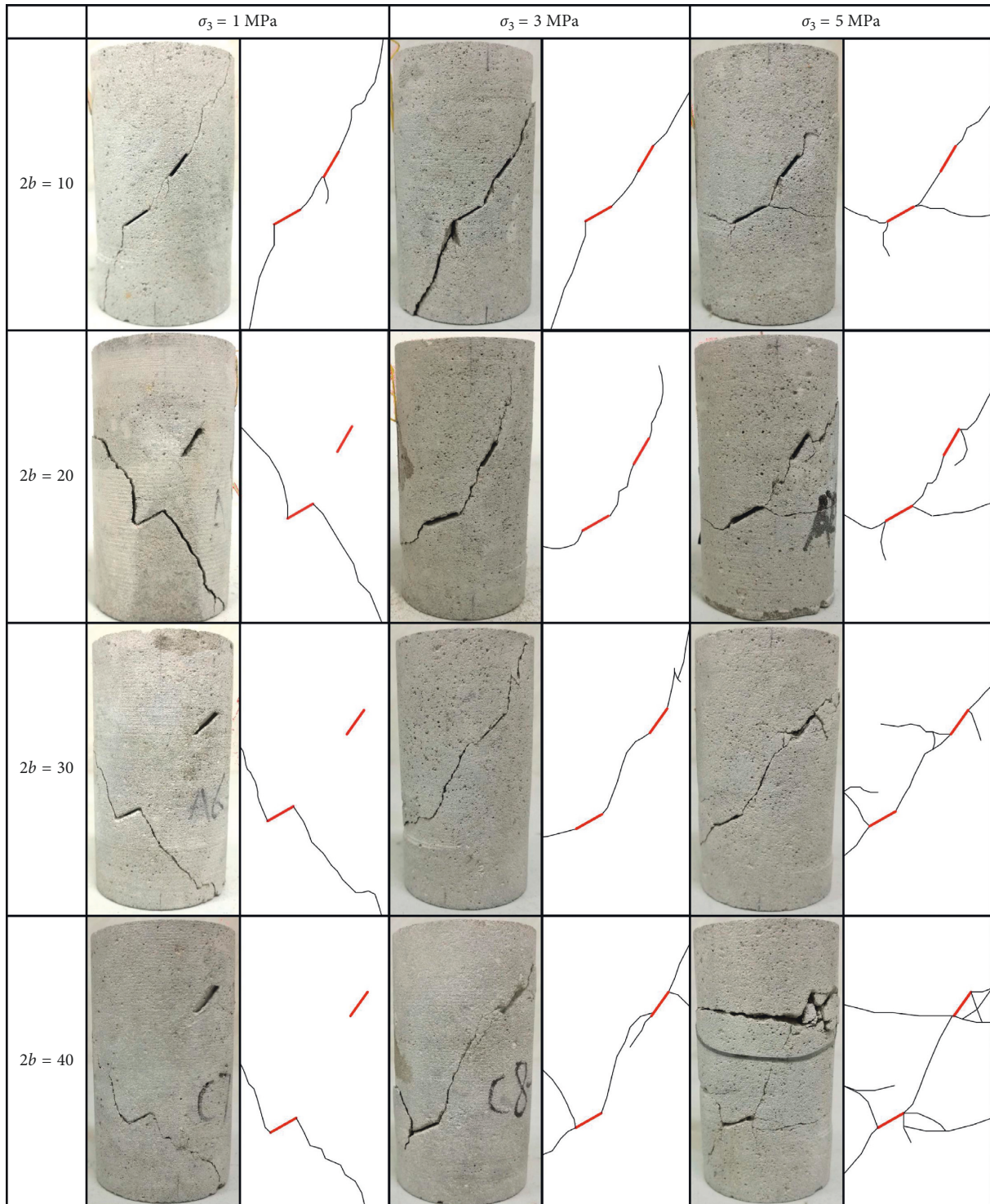
FIGURE 6: Failure modes of the specimens with a geometry of 2b-30-60-60 but with different bridge lengths.

that the change in α_1 affects the coalescence pattern when the bridge length increased from 10 mm to 20 mm. For the specimens with a geometry of 30-30-60-60, no coalescence was observed under the confining pressure of 1 MPa. When the confining pressure was 3 MPa, the coalescence type was type 5 and the failure mode was tensile-shear failure. The coalescence type was type 3, and the failure mode was shear failure under the confining pressure of 5 MPa. For the

specimens with a geometry of 40-0-60-60, when the confining pressure was 1 MPa and 3 MPa, the failure mode and coalescence pattern of the specimens were the same as those of specimens with a geometry of 30-30-60-60. Type 5 coalescence was observed when the confining pressure was 5 MPa. In addition, many cracks were seen, and a normal shear crack that initiated from the inner tip of the specimen was the main cause of shear failure of the specimens.
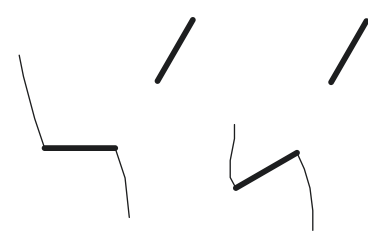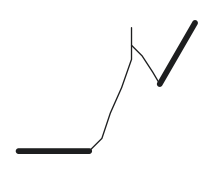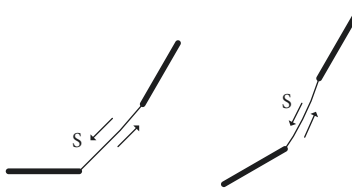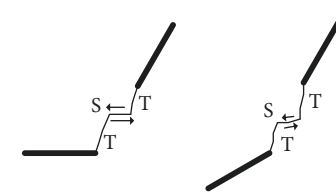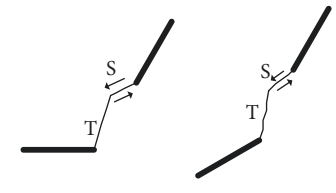
Category	Coalescence patterns for specimens having different bridge lengths	Crack types involved
1		No coalescence
2		Indirect coalescence by two cracks (crack types vary)
3		Shear crack
4		Two tensile crack and one shear crack segments between inner flaw tips
5		One tensile crack and one shear crack segments between inner flaw tips

FIGURE 7: Types of coalescence in triaxial compression for specimens with geometries of 2b-0-60-60 and specimens 2b-30-60-60 with different bridge lengths.

Figure 6 shows that no coalescence was observed under a confining pressure of 1 MPa, and that failure of all specimens was caused by an antitensile crack, except for specimens with a bridge length of 10 mm.

Figures 5 and 6 show that, under a low confining pressure (1 MPa), the coalescence pattern changed from coalescence to no coalescence with the increase of bridge length, and it proves that the interaction between flaws becomes weaker. Under a high confining pressure (5 MPa), coalescence of cracks was observed in all specimens, which shows that an increase in the confining pressure increased the interaction between flaws. From Figures 5 and 6, it can be seen that, the larger the confining pressure, the easier for the shear crack to initiate, and the easier for the shear failure of the specimens to occur. In general, under the condition of the same bridge length and confining pressure, the types of coalescence for specimens with geometries of 2b-0-60-60 and 2b-30-60-60 were different. However, the failure modes for the specimens with geometries of 2b-0-60-60 and 2b-0-60-60 were similar, which indicates that the increase in α_1

from 0° to 30° had an influence on the coalescence patterns but had little effect on failure modes.

3.3. Effect of Bridge Inclination Angle on the Cracking Process, Coalescence Pattern, and Failure Mode.

Figures 8 and 9 show failure modes of the specimens with geometries of 20-0-60-β and 20-30-60-β and different bridge angles under 1 MPa, 3 MPa, and 5 MPa. Figure 10 shows the coalescence types for these specimens. Figure 8 shows that, for specimens with a geometry of 20-0-60-0 under a confining pressure of 1 MPa, tensile cracks initiated from the inner tips of flaw 1 and flaw 2, no coalescence occurred in the bridge region, and the failure mode of the specimens was tensile-shear failure. Under a confining pressure of 3 MPa and 5 MPa, normal shear crack coalesced two inner tips of flaw 1 and flaw 2, the type of coalescence is type 8 (as shown in Figure 10), and failure mode was shear failure. For the specimens with a geometry of 20-0-60-30, no coalescence was observed under a confining pressure of 1 MPa and 3 MPa, and the failure mode was tensile-shear failure. However, with a confining pressure of 5 MPa, the type of coalescence was type 8, and the rock bridge was cut through by a shear crack. The above description shows that, for a specimen with a small bridge inclination angle, no crack coalesced two inner tips of the preexisting flaws under a relative low confining pressure; however, normal shear crack coalesced two inner tips of the preexisting flaws under a relative high confining pressure and induced horizontal failure plane. Coalescence type 9 occurred for specimens with a geometry of 20-0-60-60 under a confining pressure of 1 MPa, but under confining pressures of 3 MPa and 5 MPa, coalescence type 10 occurred. The failure modes of specimens with a geometry of 20-0-60-60 were identical (tensile-shear failure) under different confining pressures. For the specimens with a geometry of 20-0-60-90 under different confining pressure, the rock bridge was cut through by tensile cracks and the type of coalescence was the same (type 7). The failure mode of tensile failure occurred in specimens with a geometry of 20-0-60-90 under confining pressures of 1 MPa and 3 MPa; however, tensile-shear failure occurred under a confining pressure of 5 MPa. When the bridge inclination angle was 120°, the projections of flaw 1 and flaw 2 on the horizontal plane overlapped, and flaw 2 had a shielding effect on flaw 1. Therefore, for the specimens with a geometry of 20-0-60-120 under different confining pressures, no coalescence was observed in the bridge region. Failure modes of the specimens with a geometry of 20-0-60-120 under the confining pressure of 1 MPa and 3 MPa was tensile-shear failure, but the failure mode under a confining pressure of 5 MPa was shear failure, which was caused by a normal shear crack emanating from the tips of flaw 1. Figure 8 shows that, under a relatively low confining pressure and with an increase in the bridge inclination angle, the coalescence pattern changed from no coalescence ($\beta = 0°$ and 30°) to coalescence caused by the linkage of shear crack and tensile crack ($\beta = 60°$), to coalescence caused by the linkage of tensile cracks ($\beta = 90°$), and to no coalescence ($\beta = 120°$). Under a

relatively high confining pressure and with an increase in the bridge inclination angle, the coalescence pattern changed from coalescence caused directly by a shear crack ($\beta = 0°$ and 30°) to coalescence caused by the linkage of shear crack and tensile crack ($\beta = 60°$), to coalescence caused by the linkage of tensile cracks ($\beta = 90°$), and to no coalescence ($\beta = 120°$). These results prove that bridge inclination angle and confining pressure had an obvious influence on both the coalescence patterns and failure modes. It can be seen from Figure 8 that there is an increased probability of a tensile crack occurring with an increase in the bridge inclination angle, and Figure 8 also shows that, for the specimens with different bridge inclination angles, shear cracks occur easily under a large confining pressure and lead to the shear failure of the specimen.

Figure 9 shows that, for the specimens with a geometry of 20-30-60-0, failure modes and coalescence patterns are the same as those of specimens with a geometry of 20-0-60-0 under the same confining pressure. It proves that, when the bridge inclination angle is 0°, the change of α_1 from 0° to 30° has little effect on the failure mode and coalescence pattern of the specimens. For the specimens with a geometry of 20-30-60-30, when the confining pressure was 1 MPa, no coalescence was observed. Under confining pressures of 3 MPa and 5 MPa, the type of coalescence was type 11, and crack coalescence eventually occurred when the shear crack initiated from the inner tip of flaw 1 connecting the antitensile crack initiated from the inner tip of flaw 2. The coalescence pattern of the specimens with a geometry of 20-30-60-30 was different from that of specimens with a geometry of 20-0-60-30, which proves that when the bridge inclination angle was 30°, the change of α_1 from 0° to 30° affected the coalescence pattern of the specimens. For the specimens with a geometry of 20-30-60-60, no coalescence was observed under a confining pressure of 1 MPa, but coalescence type 9 was observed under confining pressures of 3 MPa and 5 MPa. With a bridge inclination angle of 90° and 120° and under different confining pressures, no coalescence occurred in the bridge region and the failure mode of specimens was antitensile cracks.

Figure 9 shows that no coalescence was observed in the specimens with five different bridge inclination angles under the confining pressure of 1 MPa. When the bridge inclination angles were 90° and 120°, no coalescence was observed in the bridge region under different confining pressures. However, Figure 8 shows that coalescence occurred in the bridge region for specimens with bridge inclination angles of 60° and 90° under a confining pressure of 1 MPa. Moreover, Figure 8 shows that coalescence was observed in specimens with a bridge inclination angle of 90° under different confining pressures, which proves that when the bridge inclination angle increases to 30°, the interaction between flaws becomes weaker, and the rock bridge is less likely to be cut through. A comparison between Figures 8 and 9 shows that when $\alpha_1 = 0°$, it was easy for a normal shear crack to initiate from the tips of flaw 1 and cause horizontal failure plane; this is because the preexisting flaw was an open flaw, and when $\alpha_1 = 0°$, there
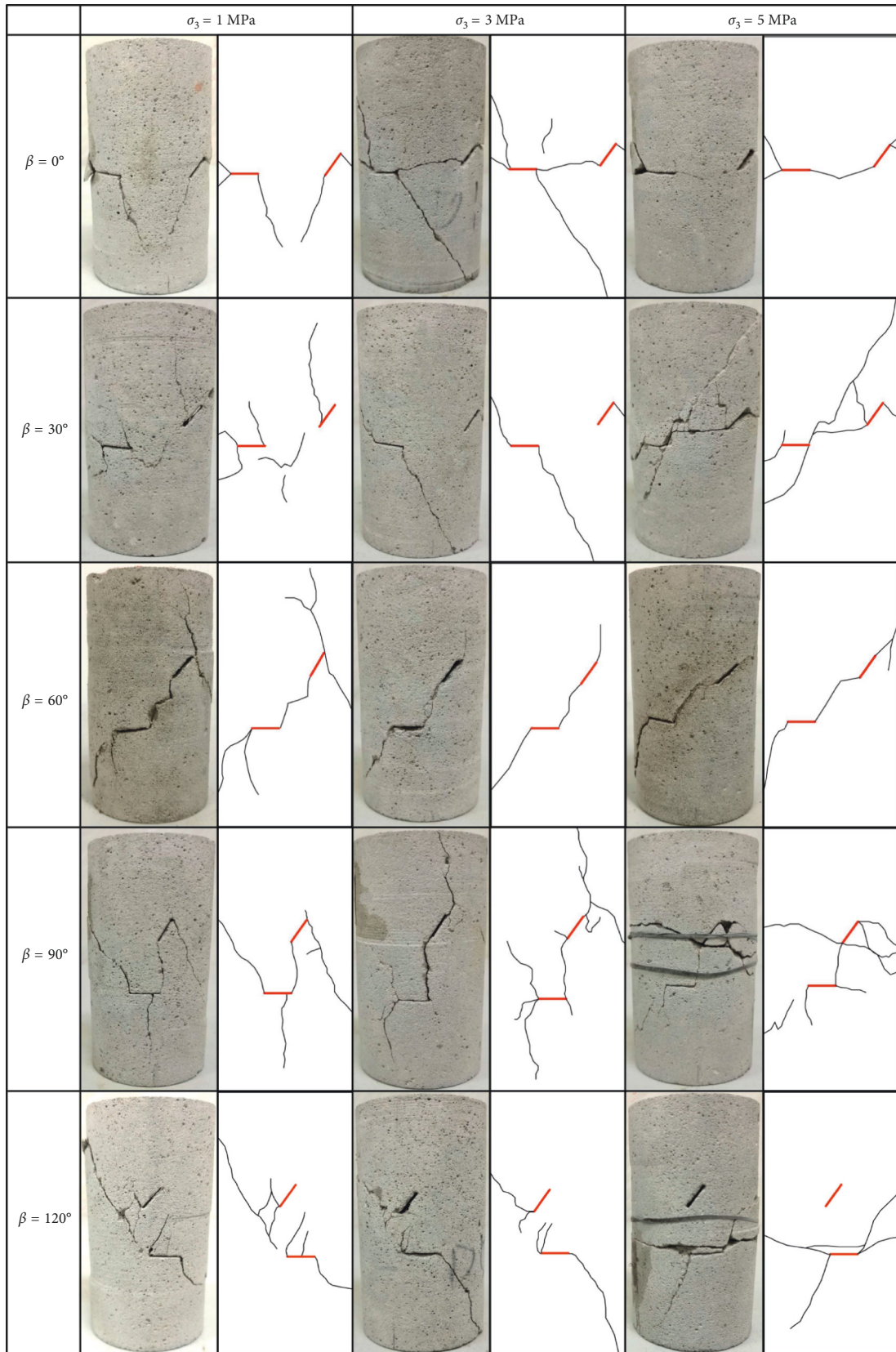
FIGURE 8: Failure modes of the specimens with a geometry of 20-0-60-β and with different bridge angles.
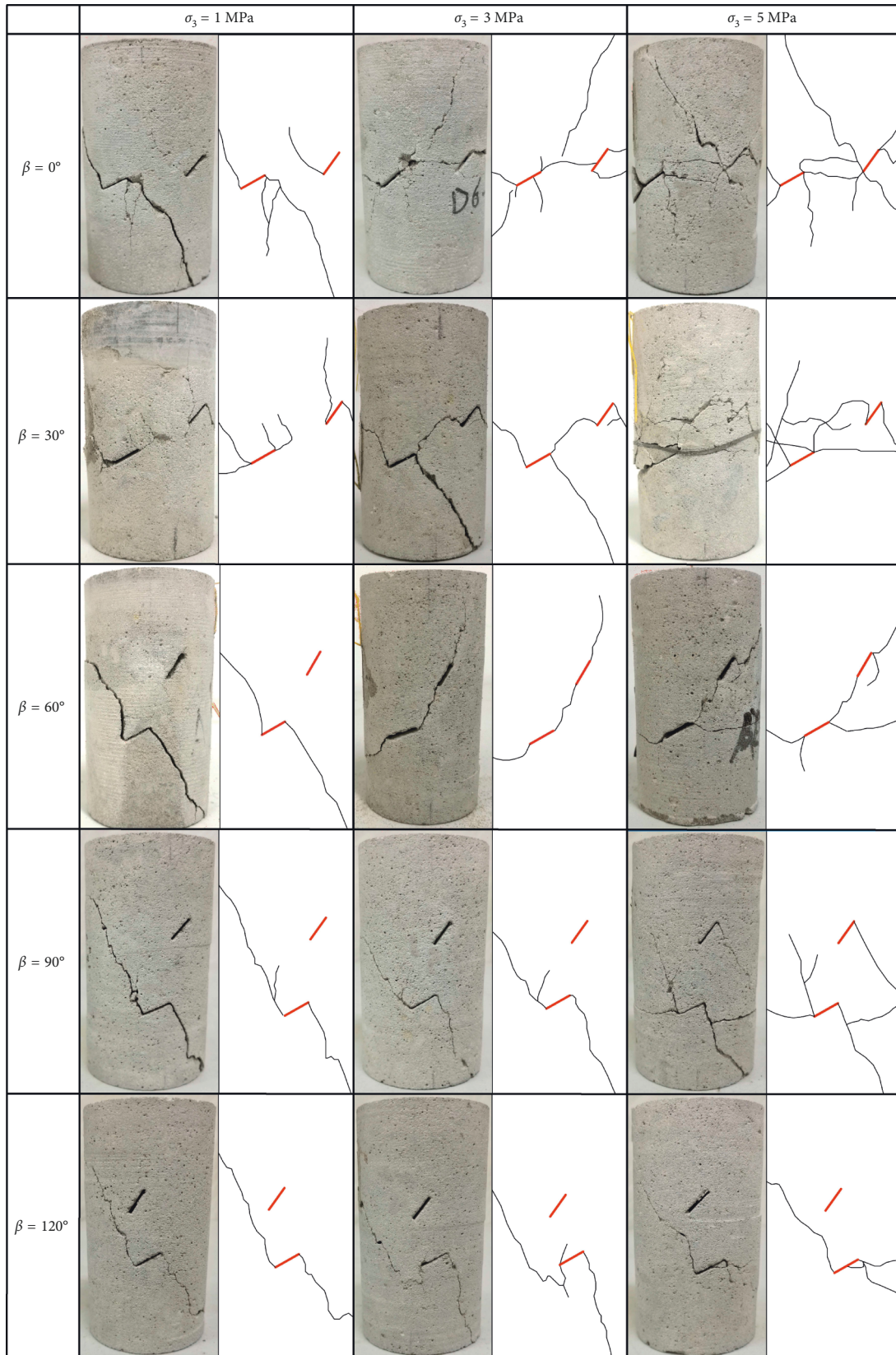
FIGURE 9: Failure modes of the specimens with a geometry of 20-30-60-β and with different bridge angles.

Category	Coalescence patterns for specimens having different bridge angles	Crack types involved
6		No coalescence
7		Tensile crack
8		Shear crack
9		Two tensile crack and one shear crack segments between inner flaw tips
10		One tensile crack and one shear crack segments between inner flaw tips
11		One antitensile crack and one shear crack segments between inner flaw tips

FIGURE 10: Types of coalescence in triaxial compression for specimens with geometries of 20-0-60-β and 20-30-60-β with different bridge angles.

was a strong stress concentration at the flaw tip, [25] and cracks emanated easily. Moreover, the tip of a flaw with an inclination angle of 0° was closer to the edge of a specimen than that of other flaw inclination angles; when a crack initiates from the tip of a flaw, it easily propagates to the edge of a specimen and causes horizontal failure plane.

When $\alpha_1 = 30°$, an antitensile crack easily initiated from the tip of flaw 1, but not a shear crack. It shows that the change of α_1 can change crack types and the coalescence pattern in the bridge region of the specimens. It is evident from Figures 8 and 9 that there were large changes in the coalescence patterns in the bridge region and the failure mode of specimens with an increase in the inclination angle from $0°$ to $120°$, which indicates that the bridge inclination angle had a significant influence on the coalescence pattern and failure mode.

From Figures 5, 6, 8, and 9, it can be seen that both the bridge length and bridge inclination angle had an influence on the coalescence pattern in the bridge region, but the influence of the bridge inclination angle was far greater than that of the bridge length. As $2b$ increased from 10 mm to 40 mm, the failure modes of specimens with a geometry of 2b-0-60-60 were almost the same as those of specimens with a geometry of 2b-30-60-60. However, as β increased from $0°$ to $120°$, the coalescence patterns and failure modes of specimens with a geometry of 20-0-60-β differed from those of specimens with a geometry of 20-30-60-β. It proves that the influence of α_1 on the coalescence patterns and failure modes of the specimens with different bridge inclination angles was larger than the influence of α_1 on specimens with different bridge lengths.

3.4. Effect of Bridge Length on Peak Strength and Shear Parameters. Figure 11(a) shows the peak strength of the specimens with a geometry of 2b-0-60-60 under different confining pressures. When the confining pressure was less than or equal to 3 MPa, the peak strength increased as $2b$ increased from 10 mm to 30 mm, and then the peak strength decreases as $2b$ increases from 30 mm to 40 mm. As the increase of bridge length, it is hard for the coalescence to occur in the bridge region; therefore, the peak strength increased as $2b$ increased from 10 mm to 30 mm. As the bridge length increased to 40 mm, the tip of the preexisting flaw was close to the edge of the specimen, and shear cracks initiating from the tips of flaw 1 and flaw 2 developed easily to the edge of the specimens due to the edge effect. Therefore, the peak strength was less than that of specimens with a bridge length of 30 mm. When the confining pressure was 3 MPa and 4 MPa, the peak strength rose as $2b$ increased from 10 mm to 20 mm, and then the peak strength dropped as $2b$ increased from 20 mm to 40 mm. It proves that, under a relatively large confining pressure, as bridge length increased to 30 mm, the failure of specimens was affected by the edge effect. It indicates that the influence of edge on the crack propagation increases as the confining pressure increases. Figure 11(b) shows the peak strength of the specimens with a geometry of 2b-30-60-60 under different confining pressures. Under five different confining pressures, the peak strength increased as $2b$ increased from 10 mm to 30 mm, and then the peak strength remained basically unchanged as $2b$ increased from 30 mm to 40 mm. It proves that there was a critical value for the bridge length. When the critical value exceeded, it can be found that the increase of the bridge length had little influence on the peak

strength of the specimens. Figures 11(a) and 11(b) show that, with confining pressures of 4 MPa and 5 MPa, the variations in peak strength with bridge length were different for specimens 2b-0-60-60 and 2b-30-60-60. This is because when $\alpha_1 = 30°$, the tips of the preexisting flaws were further from the edge than with $\alpha_1 = 0°$, and they were less affected by the edge effect. Figure 11 shows that the peak strength is higher when the confining pressure is greater, and this is not dependent on flaw geometry.

Figure 12 shows the shear parameters of the specimens with geometries of 2b-0-60-60 and 2b-30-60-60, for which the internal frictional angle increases with an increase in the bridge length from 10 mm to 20 mm and then decreases with an increase in the bridge length from 20 mm to 40 mm. For the specimens with a geometry of 2b-30-60-60, the cohesion increases as the bridge length increases. However, for the specimens with a geometry of 2b-0-60-60, there were no obvious changing cohesion laws with respect to bridge length, due to the double influence of the bridge length and the edge effect on specimen failure.

3.5. Effect of Bridge Inclination Angle on Peak Strength and Shear Parameter. Figure 13 shows the peak strength of the specimens with geometries of 20-0-60-β and 20-30-60-β under different confining pressures. The variation of the peak strength with the bridge inclination angle in Figure 13(a) is similar to that in Figure 13(b), and it shows that the increase of α_1 from $0°$ to $30°$ has little effect on the change law of the peak strength with the bridge inclination angle. From Figure 13, it can be seen that the peak strength decreases as β increases from $0°$ to $60°$ and then increases as β increases from $60°$ to $120°$. Under different confining pressures, the peak strength of the specimens with $\beta = 60°$ is lowest and that of specimens with $\beta = 120°$ is largest. This is because when $\beta = 60°$, the angle between the macroscopic failure surface and the horizontal direction is approximately $45° + \varphi/2$, and the inner tips of the two preexisting flaws are on the potential failure surface of the specimen. At this time, the damage degree of the two preexisting flaws to the specimen is the greatest. When $\beta = 120°$, horizontal projections of two preexisting flaws overlap. Flaw 2 has a shielding effect on flaw 1, and the effective damage area caused by the two preexisting flaws is relatively small in the specimens with $\beta = 120°$, which makes the specimens show a higher peak strength.

Figure 14 shows the shear parameters of the specimens with geometries of 20-0-60-β and 20-30-60-β. The variation of cohesion and internal friction angle with the bridge inclination angle is not linear, and the changing law is complex. For the specimens with geometries of 20-0-60-β and 20-30-60-β, cohesion is relatively large when $\beta = 0°$ and $60°$, and the internal frictional angle is relatively large when $\beta = 90°$.

4. Conclusions

Rock-like specimens containing two unparallel flaws with varying flaw geometries were prepared, and triaxial
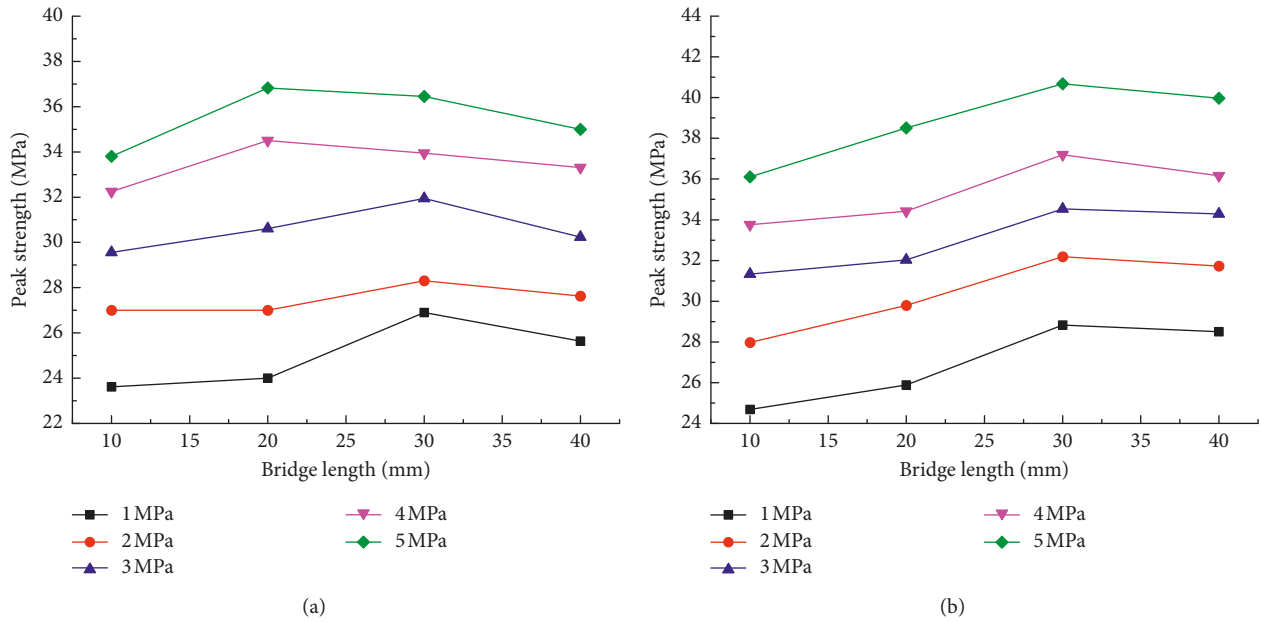
FIGURE 11: Peak strength of the specimens (a) 2*b*-0-60-60 and (b) 2*b*-30-60-60 having different bridge lengths.
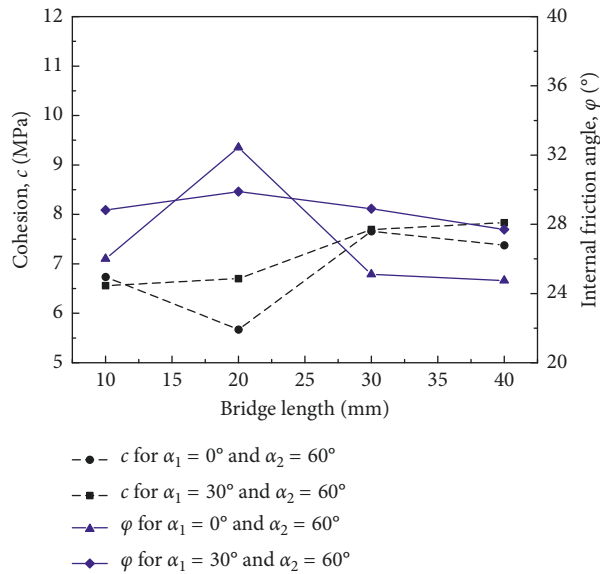

FIGURE 12: Shear parameters of the specimens 2*b*-0-60-60 and 2*b*-30-60-60 having different bridge lengths.

compressive tests were conducted to investigate the cracking behavior and mechanical properties of the precracked specimens. The following conclusions are obtained from the test results in this study:

(1) Under a low confining pressure (1 MPa), as bridge length increases, the coalescence pattern changed from different types of coalescence to no coalescence. It indicates that the interaction between the two preexisting flaws weakened as the bridge length increases. Under a high confining pressure (5 MPa), coalescence in the bridge region was observed in all the specimens, which proves that the coalescence

pattern and the failure mode of the specimens were affected by the confining pressure. When the confining pressure was low, the coalescence pattern and the failure mode of the specimens were greatly affected by the length and inclination angle of the rock bridge. When the confining pressure increased to a certain extent, the effect of the confining pressure was larger than the influence of flaw geometry, and the failure mode of specimens changed to shear failure.

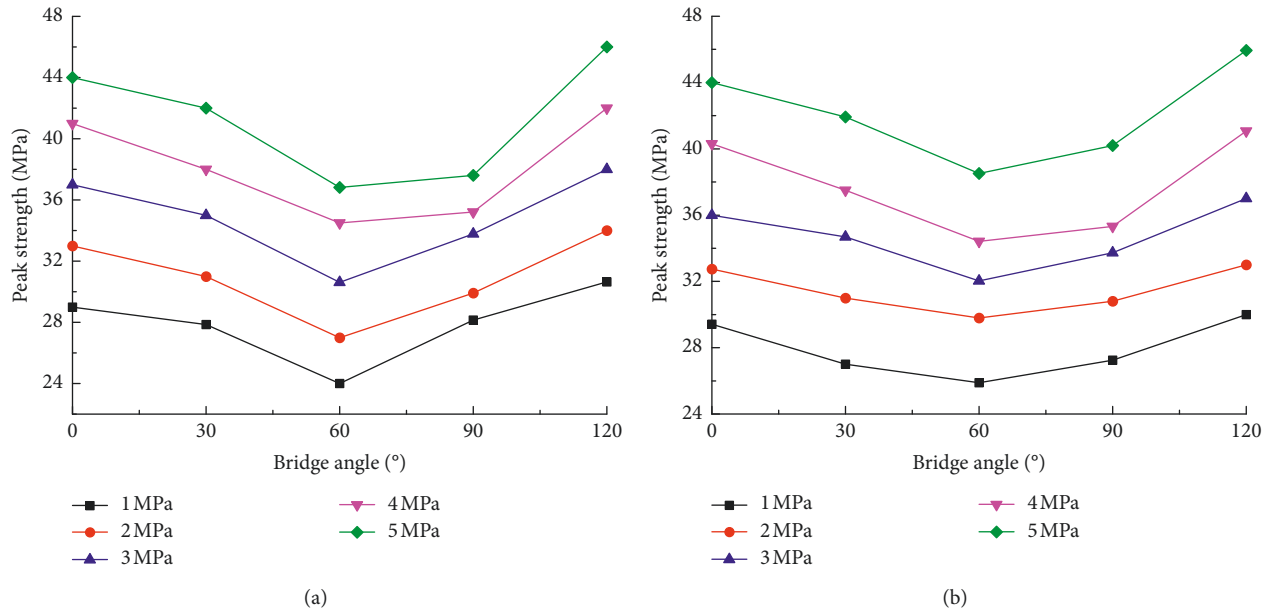(2) Both the bridge length and the bridge inclination angle had an influence on the coalescence pattern of

(a)

(b)

FIGURE 13: Peak strength of the specimens (a) 20-0-60-β and (b) 20-30-60-β having different bridge angles.
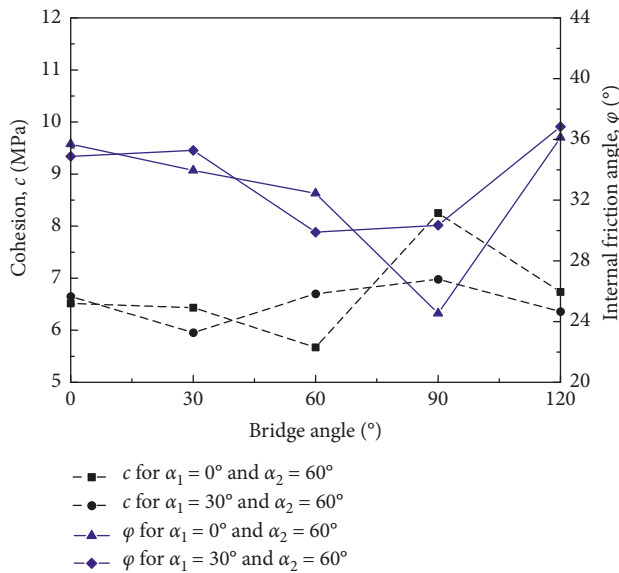

FIGURE 14: Shear parameters of the specimens 20-0-60-β and 20-30-60-β having different bridge angles.

specimens, but the influence of bridge inclination angle was much larger than the influence of bridge length. As the bridge inclination angle increased, the probability of the occurrence of tensile cracks increased.

(3) For the specimens with different bridge inclination angles, the increase in α_1 from 0° to 30° had an obvious influence on the coalescence pattern of the specimens. However, for the specimens with different bridge lengths, the increase in α_1 from 0° to 30° had a relatively small influence on the coalescence pattern.

(4) The increase in α_1 from 0° to 30° had little influence on the variation in peak strength with the bridge inclination angle. Under different confining pressures, the peak strength of the specimens with $\beta = 120°$ was the highest and that of specimens with $\beta = 60°$ was the lowest. The bridge length has a critical value, and when it is larger than the critical value, growth of the bridge length has little effect on the peak strength of samples. However, regardless of the length and inclination angle of the rock bridge, the peak strength of specimens increased with an increase in the confining pressure.

Data Availability

The data used to support the findings of this study are available from the corresponding author upon request.

Conflicts of Interest

The authors declare that they have no conflicts of interest.

Acknowledgments

References

[1] E. Z. Lajtai, "Brittle fracture in compression," *International Journal of Fracture*, vol. 10, no. 4, pp. 525–536, 1974.

[2] X. Fan, R. chen, H. Lin, H. Lai, C. Zhang, and Q. Zhao, "Cracking and failure in rock specimen containing combined flaw and hole under uniaxial compression," *Advances in Civil Engineering*, vol. 2018, Article ID 9818250, 15 pages, 2018.

[3] M. Sagong and A. Bobet, "Coalescence of multiple flaws in a rock-model material in uniaxial compression," *International Journal of Rock Mechanics and Mining Sciences*, vol. 39, no. 2, pp. 229–241, 2002.

[4] Y.-P. Li, L.-Z. Chen, and Y.-H. Wang, "Experimental research on pre-cracked marble under compression," *International Journal of Solids and Structures*, vol. 42, no. 9-10, pp. 2505–2516, 2005.

[5] L. N. Y. Wong and H. H. Einstein, "Crack coalescence in molded gypsum and carrara marble: part 1—macroscopic observations and interpretation," *Rock Mechanics and Rock Engineering*, vol. 42, no. 3, pp. 475–511, 2009.

[6] L. N. Y. Wong and H. H. Einstein, "Crack coalescence in molded gypsum and carrara marble: part 2—microscopic observations and interpretation," *Rock Mechanics and Rock Engineering*, vol. 42, no. 3, pp. 513–545, 2009.

[7] H. Lee and S. Jeon, "An experimental and numerical study of fracture coalescence in pre-cracked specimens under uniaxial compression," *International Journal of Solids and Structures*, vol. 48, no. 6, pp. 979–999, 2011.

[8] S.-Q. Yang and H.-W. Jing, "Strength failure and crack coalescence behavior of brittle sandstone samples containing a single fissure under uniaxial compression," *International Journal of Fracture*, vol. 168, no. 2, pp. 227–250, 2011.

[9] X. P. Zhang and L. N. Y. Wong, "Cracking processes in rock-like material containing a single flaw under uniaxial compression: a numerical study based on parallel bonded-particle model approach," *Rock Mechanics and Rock Engineering*, vol. 45, no. 5, pp. 711–737, 2012.

[10] Y. Zhao, L. Zhang, W. Wang, C. Pu, W. Wan, and J. Tang, "Cracking and stress-strain behavior of rock-like material containing two flaws under uniaxial compression," *Rock Mechanics and Rock Engineering*, vol. 49, no. 7, pp. 2665–2687, 2016.

[11] D. Huang, D. Gu, C. Yang, R. Huang, and G. Fu, "Investigation on mechanical behaviors of sandstone with two preexisting flaws under triaxial compression," *Rock Mechanics and Rock Engineering*, vol. 49, no. 2, pp. 375–399, 2016.

[12] S. Q. Yang, Y. Z. Jiang, W. Y. Xu, and X. Q. Chen, "Experimental investigation on strength and failure behavior of pre-cracked marble under conventional triaxial compression," *International Journal of Solids and Structures*, vol. 45, no. 17, pp. 4796–4819, 2008.

[13] Y. H. Huang and S. Q. Yang, "Mechanical and cracking behavior of granite containing two coplanar flaws under conventional triaxial compression," *International Journal of Damage Mechanics*, vol. 28, no. 4, pp. 590–610, 2018.

[14] J. Liu, Z. Zhu, and B. Wang, "The fracture characteristic of three collinear cracks under true triaxial compression," *Scientific World Journal*, vol. 2014, Article ID 459025, 5 pages, 2014.

[15] H. Haeri, K. Shahriar, M. F. Marji, and P. Moarefvand, "Experimental and numerical study of crack propagation and coalescence in pre-cracked rock-like disks," *International Journal of Rock Mechanics and Mining Sciences*, vol. 67, pp. 20–28, 2014.

[16] Y. H. Huang, S. Q. Yang, and J. Zhao, "Three-dimensional numerical simulation on triaxial failure mechanical behavior of rock-like specimen containing two unparallel fissures," *Rock Mechanics and Rock Engineering*, vol. 49, no. 12, pp. 4711–4729, 2016.

[17] S.-Q. Yang, X.-R. Liu, and H.-W. Jing, "Experimental investigation on fracture coalescence behavior of red sandstone containing two unparallel fissures under uniaxial compression," *International Journal of Rock Mechanics and Mining Sciences*, vol. 63, pp. 82–92, 2013.

[18] H. Haeri, K. Shahriar, M. F. Marji, and P. Moarefvand, "On the strength and crack propagation process of the pre-cracked rock-like specimens under uniaxial compression," *Strength of Materials*, vol. 46, no. 1, pp. 140–152, 2014.

[19] Y. Huang, S. Yang, Y. Ju, X. Zhou, and F. Gao, "Experimental study on mechanical behavior of rock-like materials containing pre-existing intermittent fissures under triaxial compression," *Chinese Journal of Geotechnical Engineering*, vol. 38, no. 7, 2016, in Chinese.

[20] P. H. S. W. Kulatilake, J. Liang, and H. Gao, "Experimental and numerical simulations of jointed rock block strength under uniaxial loading," *Journal of Engineering Mechanics*, vol. 127, no. 12, pp. 1240–1247, 2001.

[21] H. Le, S. Sun, P. H. S. W. Kulatilake, and J. Wei, "Effect of grout on mechanical properties and cracking behavior of rock-like specimens containing single flaw under uniaxial compression," *International Journal of Geomechanics*, vol. 18, no. 10, article 04018129, 2018.

[22] M. Sagong, D. Park, J. Yoo, and J. S. Lee, "Experimental and numerical analyses of an opening in a jointed rock mass under biaxial compression," *International Journal of Rock Mechanics and Mining Sciences*, vol. 48, no. 7, pp. 1055–1067, 2011.

[23] X. Chen, Z. Liao, and X. Peng, "Deformability characteristics of jointed rock masses under uniaxial compression," *International Journal of Mining Science and Technology*, vol. 22, no. 2, pp. 213–221, 2012.

[24] H. Le, S. Sun, and J. Wei, "Influence of types of grouting materials on compressive strength and crack behavior of rocklike specimens with single grout-infilled flaw under axial loads," *Journal of Materials in Civil Engineering*, vol. 31, no. 1, 2019.

[25] M. Jiang, H. Chen, N. Zhang, and R. Fang, "Distinct element numerical analysis of crack evolution in rocks containing pre-existing double flaw," *Rock and Soil Mechanics*, vol. 35, no. 11, pp. 3259–3268, 2014, in Chinese.